

1 $\delta^{13}\text{C}$ and $\delta^{37}\text{Cl}$ isotope fractionation to characterize
2 aerobic vs. anaerobic degradation of
3 trichloroethylene

4 *Almog Gafni*¹, *Christina Lihl*², *Faina Gelman*³, *Martin Elsner*^{2,4} and *Anat Bernstein*^{1*}

5

6 1 Zuckerberg Institute for Water Research, Department of Environmental Hydrology and
7 Microbiology, Ben-Gurion University of the Negev, Sede Boqer Campus, 84990, Israel

8 2 Institute of Groundwater Ecology, Helmholtz Zentrum München, Ingolstädter Landstrasse 1,
9 85764 Neuherberg, Germany

10 3 Geological Survey of Israel, 30 Malkhei Israel St., Jerusalem, 95501, Israel

11 4 Chair of Analytical Chemistry and Water Chemistry, Technical University of Munich,
12 Marchioninistrasse 17, D-81377 Munich, Germany

13

14 * Corresponding Author. E-mail address: anatbern@bgu.ac.il

15 KEYWORDS Isotope effect, groundwater contamination, natural attenuation, bioremediation

16

17 Published as **A. Gafni, Ch. Lihl, F. Gelman, M. Elsner, A. Bernstein**, $\delta^{13}\text{C}$ and $\delta^{37}\text{Cl}$ Isotope
18 Fractionation To Characterize Aerobic vs Anaerobic Degradation of Trichloroethylene, **Environ.**
19 **Sci. Technol. Lett.** **5** (2018), pp. 202-208, DOI: 10.1021/acs.estlett.8b00100

20 ABSTRACT

21 Trichloroethylene (TCE) is a carcinogenic organic chemical impacting water resources
22 worldwide. Its breakdown by reductive vs. oxidative degradation involves different types of
23 chemical bonds. Hence, if distinct isotope effects are reflected in dual element (carbon and
24 chlorine) isotope values, such trends could help distinguishing both processes in the environment.
25 This work explored dual element isotope trends associated with TCE oxidation by two pure
26 bacterial cultures: *Pseudomonas putida* F1 and *Methylosinus trichosporium* OB3b, where the latter
27 expresses either soluble methane-monooxygenase (sMMO) or particulate methane-
28 monooxygenase (pMMO). Carbon and chlorine isotope enrichment factors of TCE ($\epsilon^{13}\text{C} = -11.5,-$
29 2.4 and -4.2‰ ; $\epsilon^{37}\text{Cl} = 0.3, -1.3$ and -2.4‰ respectively) differed strongly between the strains. The
30 dual element isotope trend for strain F1 ($\epsilon^{13}\text{C}/\epsilon^{37}\text{Cl} = -38$) reflected, as expected, primary carbon
31 and negligible chlorine isotope effects, whereas unexpectedly large chlorine isotope effects
32 became apparent in the trend obtained with strain OB3b ($\epsilon^{13}\text{C}/\epsilon^{37}\text{Cl} = +1.7$ for sMMO and
33 pMMO). Therefore, although dual element isotope analysis partly reflects predicted differences in
34 oxidative vs. reductive ($\epsilon^{13}\text{C}/\epsilon^{37}\text{Cl} = 3.4$ to 5.7) degradation, the unexpected OB3b fractionation
35 data may challenge field interpretation.

36

37

38 **Introduction**

39 Aliphatic chloro-organic compounds of anthropogenic origin, among them trichloroethylene
40 (TCE), threaten the quality of water resources worldwide ^{1,2}. TCE is a volatile organic compound
41 used primarily as an industrial solvent in metal and textile industry. Due to its high density and
42 low solubility, TCE spills may move downwards in the subsurface to lower permeability layers,

43 forming pool(s) of dense non-aqueous phase liquids³ which can serve as a source of contamination
44 spread⁴. TCE is toxic and carcinogenic to humans⁵, and its drinking water concentration limit is
45 set by the EPA to 5 µg/l⁶.

46 Biodegradation is regarded as an essential component of plume remediation, where two main
47 processes may be responsible at TCE-contaminated sites: anaerobic reductive dechlorination and
48 aerobic co-metabolism⁷. Anaerobic reductive dechlorination has been extensively investigated<sup>7-
49 11</sup>. In this process TCE serves as an electron acceptor in the respiratory chain and hydrogen as an
50 electron donor. The hydrogen atoms sequentially replace chlorine atoms (“hydrogenolysis”) from
51 tetrachloroethylene (PCE), through TCE, *cis*-dichloroethylene (cDCE) and vinyl chloride (VC)
52 down to ethylene, where the lower chlorinated transformation products tend to be of greater
53 toxicity than TCE¹². The oxidative pathway, in contrast, leads to degradation products of lower
54 toxicity than VC until full mineralization (CO₂, Cl⁻) is achieved. Thus, the two differ in their
55 environmental toxicities¹³. The oxidative pathway can proceed co-metabolically, where TCE is
56 being degraded fortuitously by monooxygenase or dioxygenase enzymes that are induced for
57 oxidation of bacterial growth substrates (“auxiliary substrates”) including, e.g., methane, ethane,
58 ammonium or aromatic hydrocarbons¹⁴. Aerobic metabolic degradation, on the other hand, was
59 rarely shown for TCE¹⁵. Since TCE oxidation normally does not lead to easily monitored
60 byproducts, it is difficult to assess this process importance at polluted sites.

61 During the last ≈15 years, compound specific isotope analysis (CSIA) has been established as
62 an important tool to demonstrate the occurrence of contaminant degradation at contaminated sites
63¹⁶. The CSIA approach is based on the fact that bonds with light isotopes are normally cleaved
64 slightly faster than bonds with heavy isotopes, resulting in a kinetic isotope effect (KIE). Thus, as
65 degradation proceeds, the remaining pool of contaminant becomes gradually enriched with heavy-

66 isotope bearing molecules ¹⁶⁻¹⁸. Consequently, a direct indication of degradation is obtained, and
67 its extent may be assessed even without the need for concentration-based mass balances ^{16,19,20}.
68 Additionally, it was demonstrated that CSIA can be used for elucidating degradation mechanisms
69 ²¹. Multi-element isotope analysis may point to specific bonds involved in the rate-limiting step of
70 a reaction and different degradation mechanisms can further be distinguished ²²⁻²⁷. Recent
71 analytical developments in Cl-CSIA, either by continuous flow gas chromatography isotope ratio
72 mass spectrometry (GC/IRMS) ²⁸ or by GC-quadrupole mass spectrometry (GC/qMS) ^{26,27,29-32}
73 have facilitated the measurement of chlorine isotope ratios in chlorinated ethylenes. It was shown
74 that reductive dechlorination can be distinguished from abiotic permanganate oxidation of TCE
75 using both carbon and chlorine isotope enrichment factors ³³. Extending this capability also for
76 microbial oxidation of TCE is desired, yet only carbon isotope effects were formerly studied,
77 whereas chlorine isotope effects are still lacking.

78 Carbon isotope enrichment factors have been reported for TCE oxidation, ranging from $\epsilon_C = -$
79 1.1 to -20.7% ³⁵⁻³⁷ and overlapping with the range of its reductive dechlorination ($\epsilon_C = -2.5$ to $-$
80 15.3% ^{25,33,34,38-41}). While mechanistic details of TCE oxidative biodegradation have been
81 investigated ⁴²⁻⁴⁴ (Scheme 1), reasons for the differences in carbon isotope enrichment factors are
82 still not understood.

83 Interpretation of CSIA could become challenging due to several different reasons, all driven
84 from the fact that the apparent isotope effect cumulates various different factors that may diverge
85 the observable isotope effect from the intrinsic isotope effect ⁴⁵⁻⁴⁷. These include membrane
86 induced equilibrium isotope effect ⁴⁸, equilibrium isotope effects on enzyme binding ^{49,50} or
87 following product branching ⁵¹. In these cases distinction e.g. between anaerobic and aerobic

88 microbial degradation processes for TCE would be more complex, but in exchange the differences
89 in dual isotope trends may provide additional mechanistic insight.

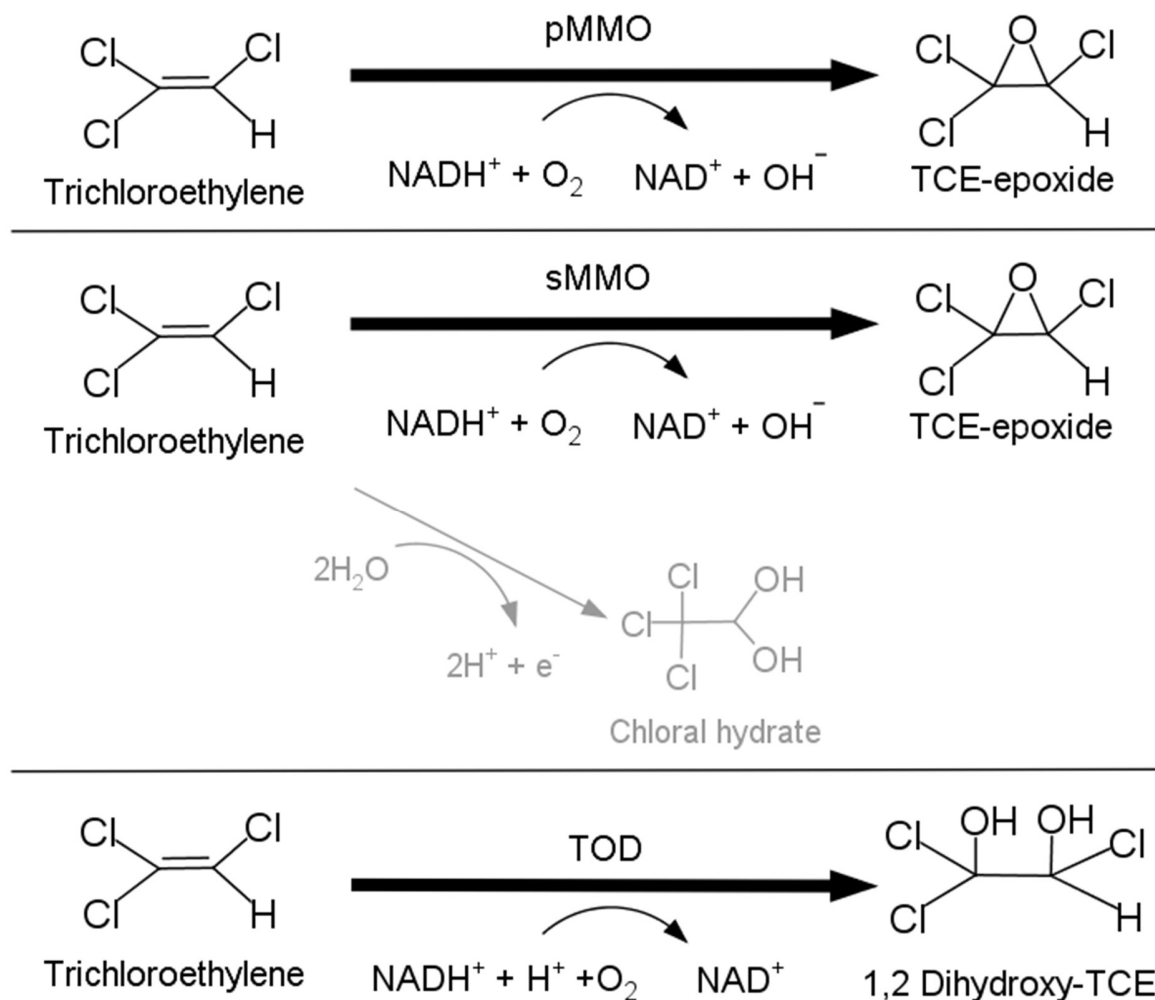
90 TCE oxidation by a monooxygenase enzyme is represented in *Methylosinus trichosporium*
91 OB3b. This widely studied strain synthesizes either soluble methane monooxygenase (sMMO)
92 soluble in the cytoplasm at low copper-to-biomass ratios^{52,53} or membrane bound particulate
93 methane monooxygenase (pMMO) when copper-to-biomass ratio increases^{54,55}. Both enzymes can
94 fortuitously mineralize TCE to CO₂⁵⁵. Fox et al⁴³, (Scheme 1) proposed that TCE degradation by
95 sMMO can occur through generation of either an epoxide or (2,2,2-Trichloroethane-1,1-diol)
96 chloral hydrate (either C=C bond epoxidation or intramolecular Cl⁻ migration). Experimentally,
97 however, chloral hydrate was shown to be a minor product⁵⁷. Furthermore, Fox et al.⁴³ did not
98 observe chloral hydrate formation by hydrolysis of authentic TCE epoxide, supporting the
99 assumption that chloral hydrate is not a degradation product of TCE epoxide.

100 TCE oxidation induced by pMMO enzyme has been studied with pMMO extracted from
101 *Methylococcus capsulatus* and whole cells of *Methylomicrobium album* Bath BG8⁴². This
102 proposed mechanism suggests TCE degradation occurs through an epoxide intermediate, similar
103 to the sMMO pathway, but with no formation of chloral hydrate.

104 TCE oxidation by a dioxygenase enzyme, finally, is represented by the toluene degrader
105 *Pseudomonas putida* F1. This strain fortuitously mineralizes TCE to CO₂ by toluene dioxygenase
106 (TDO). It was previously postulated that the rate-determining step of the reaction is a cleavage of
107 the carbon double bond, creating a dihydroxy-TCE intermediate⁴⁴.

108 In the present study we aimed to explore dual ³⁷Cl and ¹³C isotopic effects associated with
109 degradation of TCE by the methanotroph OB3b (expressing either pMMO or sMMO enzymes)
110 and the toluene degrader *Pseudomonas putida* F1. An additional objective of the study was to

111 evaluate to what extent dual carbon – chlorine isotope data can be used for distinguishing anaerobic
 112 and aerobic biodegradation of TCE in the field.



113 **Scheme 1.** Proposed rate limiting step at TCE oxidation by (upper) pMMO enzyme resulting in
 114 epoxide ⁴². (middle) sMMO enzyme resulting in epoxide and chloral hydrate formation (minor
 115 product marked gray), with the later as a minor product ⁴³ (lower) TDO enzyme ⁴⁴ resulting in
 116 1,2-Dihydroxy-TCE.

117

118 **Materials and Methods**

119 **Experimental setup**

120 Two pure strains were used in batch experiments: *Pseudomonas putida* F1 and *Methylosinus*
121 *trichosporium* OB3b. Strains were kindly provided by Prof. Lawrence P. Wackett, University of
122 Minnesota, and Dr. Jeremy Semrau, University of Michigan. The growth media for F1 was
123 prepared as described previously³⁵ and amended with trace element⁵⁸. OB3b was cultivated in
124 liquid media as described previously⁵⁹ with or without CuSO₄ for either pMMO or sMMO
125 expression, respectively. More details on the growth conditions are provided in the Supporting
126 Information.

127 Pure cultures were harvested by centrifugation and re-suspended in fresh growth media. Fresh
128 media was amended with resazurin as redox indicator (1 mg/l), TCE (5.8 mg/l), and either ethanol
129 (158 mg/l) or potassium formate (0.02 M) as NADH source for F1 or OB3b, respectively. Growth
130 media was led to equilibrate overnight on a magnetic stirrer prior inoculation. For initiating the
131 experiments, one milliliter of harvested bacteria was transferred into 60 ml autoclaved serum
132 bottles. Growth media was then added (1:5 liquid to air) maintaining a large headspace for
133 sufficient oxygen in the system and bottles were immediately crimped with a Viton septa. All
134 experiments were conducted in triplicates, and accompanied by abiotic and biotic controls (see
135 SI). Halting the degradation process was done by adding phosphoric acid (98%) to each bottle, to
136 reach pH ≤ 2. Once the experiment was completed, final TCE concentrations were measured in
137 each bottle by GC/MS (Trace 1310 coupled to a ISQ LT, Thermo Fisher Scientific). The growth
138 media was divided into glass vials, sealed with Teflon lined septa, and preserved frozen⁶⁰. Frozen
139 samples from F1 and sMMO experiments were distributed between the Geological Survey of Israel
140 and the Helmholtz Zentrum München for comparison of chlorine isotope measurements. Chloral

141 hydrate formation was monitored on a separate experiment following MTBE liquid-liquid
142 extraction modified from Nikolaou et al. ⁶¹ and GC/MS analysis (see SI for more detailed
143 description).

144 **Isotope analysis**

145 Chlorine isotope analysis was done by two different methods: (i) GC/IRMS at the Helmholtz
146 Zentrum München ³⁰ and (ii) GC/MS at the Geological Survey of Israel. For the later, six ions
147 were monitored (m/z 60, 62, 95, 97, 130 and 132), and data was evaluated following Sakaguchi-
148 Söder et al ³². Calibrating the $\delta^{37}\text{Cl}$ measurements by GC/MS to the SMOC scale was achieved
149 using three $\delta^{37}\text{Cl}$ differing in-house standards (see SI) that were isotopically characterized by GC-
150 IRMS relative to known EIL-1 and EIL-2 ³⁰ standards .

151 Carbon isotope analysis was done by GC-IRMS (either Delta-V or MAT-253, Thermo Fisher
152 Scientific). More details on the isotope analysis methods are found in the SI.

153 **Calculations**

154 TCE isotope ratios measured by either GC/IRMS or GC/qMS are reported using the delta
155 notation (eq 1):

$$156 \quad (1) \delta^h E_{sample} = \frac{R_{sample}}{R_{standard}} - 1$$

157
158 where R is the isotope ratio of carbon ($^{13}\text{C}/^{12}\text{C}$) or chlorine ($^{37}\text{Cl}/^{35}\text{Cl}$), respectively. Since
159 variations of isotope ratios are often small, the δ -values are expressed on a per mill scale.

160 To determine carbon or chlorine isotope enrichment factors (ϵ) along TCE oxidation, a modified
161 Rayleigh equation was used (eq 2):

$$162 \quad (2) \ln \frac{R_t}{R_0} = \epsilon \times \ln(f)$$

163

164 where R_0 and R_t are isotope ratios of the beginning and during degradation, respectively, and f is
165 the remaining fraction of non-degraded TCE.

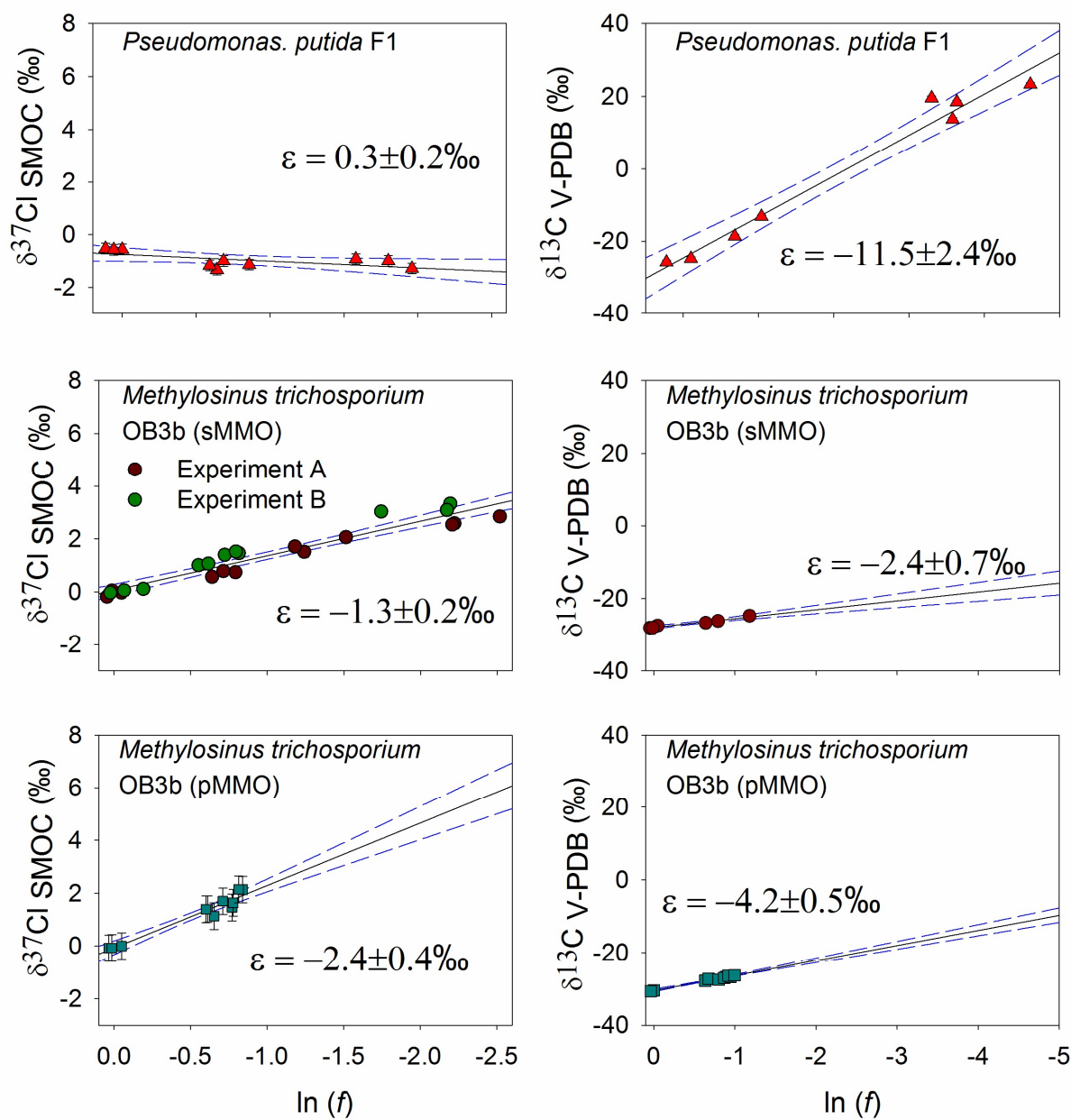
166

167 **Results and Discussions**

168 **Isotope enrichment factors and degradation mechanism**

169 Chlorine isotope analysis along TCE oxidation was carried out by GC/IRMS and by GC/qMS.
170 Both techniques resulted in $\epsilon^{37}\text{Cl}$ values that are not significantly different (Table S1). Oxidation
171 of TCE by strain F1 resulted in a negligible chlorine isotope enrichment factor ($\epsilon^{37}\text{Cl}=0.3\pm 0.2\%$)
172 along with a strong carbon isotope enrichment factor ($\epsilon^{13}\text{C}=-11.5\pm 2.4\%$) (Figure 1). The $\epsilon^{13}\text{C}$
173 value is in good agreement with earlier reported values for this strain ($\epsilon^{13}\text{C}=-13.8\pm 1.6\%$)³⁷, as
174 well as with theoretical expectations from similar experiments ($\epsilon^{13}\text{C}=-11\%$ as average over both
175 C atoms)⁶².

176 The negligible isotope enrichment along TCE oxidation by strain F1 suggest that carbon-
177 chlorine bonds are not involved in the rate-limiting step of the reaction, in line with the accepted
178 mechanistic pathway (Scheme 1). This is also in agreement with previously reported values along
179 VC and *cis*-DCE oxidation ($\epsilon^{37}\text{Cl}\approx -0.3\%$)⁶³. Likewise, negligible chlorine isotope enrichment
180 values were reported for TCE oxidation by permanganate ($\epsilon^{37}\text{Cl}=0.1\pm 0.1\%$)³³.



181
 182 **Figure 1.** Chlorine (left) and carbon (right) and isotope composition of TCE oxidized by TDO
 183 (strain F1), pMMO (strain OB3b), or sMMO (strain OB3b). Dashed lines represent 95%
 184 confidence intervals and the error bars represent the uncertainty of the method ($\pm 0.5\text{‰}$ for ^{13}C -
 185 IRMS and ^{37}Cl -GC/MS and ± 0.2 for ^{37}Cl -IRMS).

186

187 Carbon isotope enrichment along TCE oxidation by strain OB3b was significantly different from
188 strain F1, in consistence with previous studies^{36,37}. Oxidation by sMMO, presented a lower carbon
189 isotope enrichment ($\epsilon^{13}\text{C}=-2.4\pm 0.7\text{‰}$) than F1, together with a comparatively pronounced chlorine
190 isotope enrichment ($\epsilon^{37}\text{Cl}=1.3\pm 0.2\text{‰}$). This pattern was reinforced by results of TCE oxidation by
191 pMMO, where both carbon ($\epsilon^{13}\text{C}=-4.2\pm 0.5\text{‰}$) and chlorine ($\epsilon^{37}\text{Cl}=-2.4\pm 0.4\text{‰}$) isotope enrichment
192 factors were twice as high compared to sMMO (Figure 1), so that the dual element isotope trend
193 remained the same.

194 Chloral hydrate was detected as a minor intermediate along TCE oxidation by sMMO, and was
195 not detected for pMMO. Since this intermediate did not accumulate in the growth medium, we
196 were unable to assess the overall magnitude of this chlorine migration route for sMMO.
197 Nevertheless, throughout the experiment chloral hydrate concentrations did not exceed 6% of the
198 initial TCE concentration (Figure S1), similar to earlier reports⁴³. If this route is significant, one
199 might speculate that the pronounced chlorine isotope enrichment may be attributable to chlorine
200 migration. However, this would not explain the pronounced ϵ value along TCE oxidation by
201 pMMO, where chloral hydrate was not detected (Scheme 1). Hence, we infer that the pronounced
202 chlorine isotope enrichment for both sMMO and pMMO is not related to chlorine migration.

203 Recently published studies reported unexpectedly large chlorine isotope enrichment values
204 along different transformation processes of chlorinated hydrocarbons. These were reported for
205 both primary⁶⁴ as well as secondary chlorine isotope effects^{34,64-66}, providing analogous
206 observations that relatively high chlorine isotope effects can be observed – like with sMMO and
207 pMMO - even though a C-Cl bond may not be cleaved in all circumstances. Future computational
208 work is needed in order to understand the underlining cause of the unexpectedly large chlorine
209 enrichment values of OB3b, in similarity to former studies on dechlorination⁶⁷.

210 Dual element isotope trends were plotted for the different enzymes reflecting similar trends for
211 sMMO and pMMO and a different trend for strain F1 (Figure 2). The sMMO and pMMO enzymes
212 differ in their metal centers ⁶⁶, degradation products (formation of chloral hydrate) ⁴² and
213 degradation rates ⁵³. Their similar dual element isotope trends (1.8 ± 0.6 and $1.7\pm 0.4\text{‰}$
214 respectively), may suggest a similar reaction mechanism ²²⁻²⁷. The different dual element isotope
215 trends observed for the strains OB3b and F1 (1.7 ± 0.4 and $-38\pm 27\text{‰}$ respectively), may either be
216 influenced by equilibrium isotope effects on binding to enzyme or a different biochemical reaction
217 mechanism. Recent publications ^{49,50} suggests that dual-element isotope slope may not necessarily
218 reflect a chemical bond conversion, but instead preceding steps prior to catalysis. However we
219 cannot exclude that the different dual element isotope slopes are due to different biochemical
220 reaction mechanisms (i.e., a different manner of bond changes).

221 **Environmental significance**

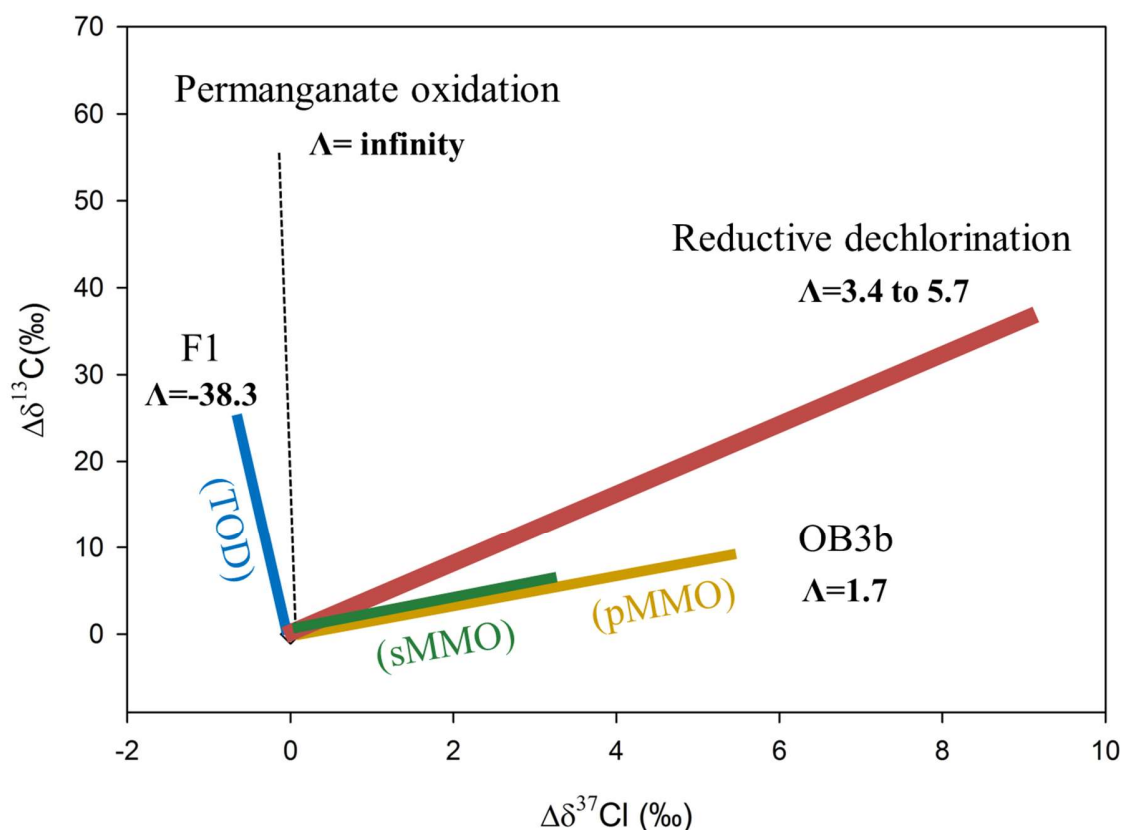
222 An attractive feature of the dual isotope approach is the possibility to distinguish between
223 transformation mechanisms in the environment. Our results show that for strain F1 as a model
224 organism, a distinction between aerobic and anaerobic degradation may indeed be possible if both
225 $\delta^{13}\text{C}$ and $\delta^{37}\text{Cl}$ values are measured (Figure 2). The observed $\epsilon^{13}\text{C}$ vs. $\epsilon^{37}\text{Cl}$ trend for TCE
226 oxidation by F1 strain is similar to permanganate oxidation ³³ and it differs significantly from
227 reported trends for biotic ^{25,33,34} and abiotic ^{25,68} reduction. This observation meets the intuitive
228 assumption that chlorine isotope enrichment along TCE oxidation should be negligible, facilitating
229 the distinction between both pathways ^{33,63}.

230 On a more refined level, the surprising differences in the dual element isotope results between
231 strain F1 and strain OB3b ($-38\pm 27\text{‰}$ vs. $1.7\pm 0.4\text{‰}$) show that this overarching mechanistic picture
232 warrants further investigation. Although both strains OB3b and F1 are thought to oxidize TCE via

233 oxidation of the double bond, they do not present similar dual element isotope trends. Moreover,
234 while the F1 dual element isotope trend is greater than the anaerobic trend, that of OB3b is smaller.
235 Thus, at first sight the dual element isotope trend observed with OB3b seems to interfere with
236 pathway distinction. However, it is important to note that the isotope enrichment is rather small
237 for strain OB3b (Figure 2) and may not necessarily lead to large misinterpretations at field sites.

238 From the environmental perspective, OB3b results indicate a surprising chlorine involvement in
239 what until now has been considered as a classical epoxidation mechanism. Further research is
240 therefore needed to determine whether the OB3b results are generally representative of
241 monooxygenase enzymes and what the relevance of this monooxygenase enzyme-catalyzed
242 pathway is for TCE oxidation at polluted sites.

243



244 **Figure 2.** Dual element isotope plot of $\delta^{13}\text{C}$ vs. $\delta^{37}\text{Cl}$ representing $\sim 90\%$ degradation. Trend-
 245 lines were shifted to the origin by presenting the change in the isotope composition ($\Delta\delta$) rather
 246 than the absolute delta values. The slope of the lines ($\Delta\delta^{13}\text{C}/\Delta\delta^{37}\text{Cl}$) corresponds approximately
 247 to the ratio $\epsilon^{13}\text{C}/\epsilon^{37}\text{Cl}$, represented as Λ . Green: *Methylosinus trichosporium* OB3b expressing
 248 sMMO; Orange: *Methylosinus trichosporium* OB3b expressing pMMO; Blue: *Pseudomonas*
 249 *putida* F1 expressing TOD. Black: abiotic permanganate oxidation ³³. Red: biotic reductive
 250 dechlorination by *Geobacter lovleyi* ²⁵, *Desulfitobacterium hafniense* Y51 ²⁵ and *Dehalococcoides*
 251 ³⁴, abiotic reductive dechlorination by zero valent iron ⁶⁸ and enzymatic cofactor cobalamin ²⁵.

252 ACKNOWLEDGMENT

253 This study was supported by the German-Israeli Foundation (GIF) grant number I-1267-
254 307.8/2014 and by the Israeli Water Authority, grant number 4501284699. AG fellowship was
255 supported by the Israeli Ministry of Science, Technology and Space, fellowship number 3-
256 13550.

257 REFERENCES

- 258 (1) Agency for Toxic Substances and Disease Registry. *Toxicological Profile for*
259 *Trichloroethylene*; 2015.
- 260 (2) European Environment Agency. *Progress in Management of Contaminated Sites*; 2014.
- 261 (3) Bourg, A. C. M.; Mouvet, C.; Lerner, D. N. A Review of the Attenuation of
262 Trichloroethylene in Soils and Aquifers. *Q. J. Eng. Geol.* **1992**, *25*, 359–370 DOI: 0481-
263 2085/92.
- 264 (4) Russell, H. H.; Matthews, J. E.; Sewell, G. W. *TCE Removal from Contaminated Soil and*
265 *Ground Water*; 1992.
- 266 (5) Chiu, W. A.; Jinot, J.; Scott, C. S.; Makris, S. L.; Cooper, G. S.; Dzubow, R. C.; Bale, A.
267 S.; Evans, M. V.; Guyton, K. Z.; Keshava, N.; Lipscomb, J. C.; Barone, S.; Fox, J. F.;
268 Gwinn, M. R.; Schaum, J.; Caldwell, J. C. *Human Health Effects of Trichloroethylene: Key*
269 *Findings and Scientific Issues*; 2012; Vol. 121.
- 270 (6) Environmental Protection Agency. *National Primary Drinking Water Regulations*; 2009.
- 271 (7) Bradley, P. M. History and Ecology of Chloroethene Biodegradation: A Review.
272 *Bioremediat. J.* **2003**, *7* (2), 81–109 DOI: 10.1080/10889860390246141.
- 273 (8) Futagami, T.; Goto, M.; Furukawa, K. Biochemical and Genetic Bases of Dehalorespiration.
274 *Chem. Rec.* **2008**, *8*, 1–12 DOI: 10.1002/tcr.20134.
- 275 (9) Maphosa, F.; de Vos, W. M.; Smidt, H. Exploiting the Ecogenomics Toolbox for

- 276 Environmental Diagnostics of Organohalide-Respiring Bacteria. *Trends Biotechnol.* **2010**,
277 28 (6), 308–316 DOI: 10.1016/j.tibtech.2010.03.005.
- 278 (10) Smidt, H.; de Vos, W. M. Anaerobic Microbial Dehalogenation. *Annu. Rev. Microbiol.*
279 **2004**, 58, 43–73 DOI: 10.1146/annurev.micro.58.030603.123600.
- 280 (11) Holliger, C.; Wohlfarth, G.; Diekert, G. Reductive Dechlorination in the Energy
281 Metabolism of Anaerobic Bacteria. *FEMS Microbiol. Rev.* **1999**, 22, 383–398 DOI:
282 10.1016/S0168-6445(98)00030-8.
- 283 (12) Kielhorn, J.; Melber, C.; Wahnschaffe, U.; Aitio, A.; Mangelsdorf, I. *Vinyl Chloride: Still*
284 *a Cause for Concern.*; 2000; Vol. 108.
- 285 (13) Mattes, T. E.; Alexander, A. K.; Coleman, N. V. Aerobic Biodegradation of the
286 Chloroethenes: Pathways, Enzymes, Ecology, and Evolution. *FEMS Microbiol. Rev.* **2010**,
287 34, 445–475 DOI: 10.1111/j.1574-6976.2010.00210.x.
- 288 (14) Suttinun, O.; Luepromchai, E.; Müller, R. Cometabolism of Trichloroethylene: Concepts,
289 Limitations and Available Strategies for Sustained Biodegradation. *Rev. Environ. Sci.*
290 *Biotechnol.* **2013**, 12 (1), 99–114 DOI: 10.1007/s11157-012-9291-x.
- 291 (15) Schmidt, K. R.; Gaza, S.; Voropaev, A.; Ertl, S.; Tiehm, A. Aerobic Biodegradation of
292 Trichloroethene without Auxiliary Substrates. *Water Res.* **2014**, 59, 112–118 DOI:
293 10.1016/j.watres.2014.04.008.
- 294 (16) Thullner, M.; Centler, F.; Richnow, H. H.; Fischer, A. Quantification of Organic Pollutant
295 Degradation in Contaminated Aquifers Using Compound Specific Stable Isotope Analysis
296 – Review of Recent Developments. *Org. Geochem.* **2012**, 42 (12), 1440–1460 DOI:
297 10.1016/j.orggeochem.2011.10.011.
- 298 (17) Elsner, M.; Zwank, L.; Hunkeler, D.; Schwarzenbach, R. A New Concept Linking

- 299 Observable Stable Isotope Fractionation to Transformation Pathways of Organic Pollutants.
300 *Environ. Sci. Technol.* **2005**, *39* (18), 6896–6916 DOI: 10.1021/es0504587.
- 301 (18) Braeckevelt, M.; Fischer, A.; Kästner, M. Field Applicability of Compound-Specific
302 Isotope Analysis (CSIA) for Characterization and Quantification of In Situ Contaminant
303 Degradation in Aquifers. *Appl. Microbiol. Biotechnol.* **2012**, *94* (6), 1401–1421 DOI:
304 10.1007/s00253-012-4077-1.
- 305 (19) Meckenstock, R. U.; Morasch, B.; Griebler, C.; Richnow, H. H. Stable Isotope Fractionation
306 Analysis as a Tool to Monitor Biodegradation in Contaminated Aquifers. *J. Contam.*
307 *Hydrol.* **2004**, *75*, 215–225 DOI: 10.1016/j.jconhyd.2004.06.003.
- 308 (20) Höhener, P. Simulating Stable Carbon and Chlorine Isotope Ratios in Dissolved
309 Chlorinated Groundwater Pollutants with BIOCHLOR-ISO Ethene Ethene Chlorine :
310 Standard Approach. *J. Contam. Hydrol.* **2016**, *195*, 52–61 DOI:
311 10.1016/j.jconhyd.2016.11.002.
- 312 (21) Aelion, C. M.; Höhener, P.; Hunkeler, D.; Aravena, R. *Environmental Isotopes in*
313 *Biodegradation and Bioremediation*; 2009.
- 314 (22) Meyer, A. H.; Penning, H.; Elsner, M. C and N Isotope Fractionation Suggests Similar
315 Mechanisms of Microbial Atrazine Transformation despite Involvement of Different
316 Enzymes (AtzA and TrzN). *Environ. Sci. Technol.* **2009**, *43* (21), 8079–8085 DOI:
317 10.1021/es9013618.
- 318 (23) Penning, H.; Sørensen, S. R.; Meyer, A. H.; Aamand, J.; Elsner, M. C, N, and H Isotope
319 Fractionation of the Herbicide Isoproturon Reflects Different Microbial Transformation
320 Pathways. *Environ. Sci. Technol.* **2010**, *44* (7), 2372–2378 DOI: 10.1021/es9031858.
- 321 (24) Bernstein, A.; Ronen, Z.; Gelman, F. Insight on RDX Degradation Mechanism by

- 322 Rhodococcus Strains Using ^{13}C and ^{15}N Kinetic Isotope Effects. *environmental Sci.*
323 *Technol.* **2013**, *47*, 479–484 DOI: 10.1021/es302691g.
- 324 (25) Cretnik, S.; Thoreson, K. A.; Bernstein, A.; Ebert, K.; Buchner, D.; Laskov, C.; Haderlein,
325 S.; Shouakar-stash, O.; Kliegman, S.; McNeill, K.; Elsner, M. Reductive Dechlorination of
326 TCE by Chemical Model Systems in Comparison to Dehalogenating Bacteria: Insights from
327 Dual Element Isotope Analysis ($^{13}\text{C}/^{12}\text{C}$, $^{37}\text{Cl}/^{35}\text{Cl}$). *environmental Sci. Technol.* **2013**,
328 *47*, 6855–6869 DOI: 10.1021/es400107n.
- 329 (26) Palau, J.; Jamin, P.; Badin, A.; Vanhecke, N.; Haerens, B.; Brouyère, S.; Hunkeler, D. Use
330 of Carbon - Chlorine Dual Isotope Analysis to Assess the Degradation Pathways of 1,1,1-
331 Trichloroethane in Groundwater. *Water Res.* **2016**, *92*, 235–243 DOI:
332 10.1016/j.watres.2016.01.057.
- 333 (27) Palsu, J.; Cretnik, S.; Shouakar-Stash, O.; Hoche, M.; Elsner, M.; Hunkeler, D. C and Cl
334 Isotope Fractionation of 1,2-Dichloroethane Displays Unique $\delta^{13}\text{C}/\delta^{37}\text{Cl}$ Patterns for
335 Pathway Identification and Reveals Surprising C–Cl Bond Involvement in Microbial
336 Oxidation. *Environ. Sci. Technol.* **2014**, *48*, 9430–9437 DOI: 10.1021/es5031917.
- 337 (28) Shouakar-Stash, O.; Drimmie, R. J.; Zhang, M.; Frape, S. K. Compound-Specific Chlorine
338 Isotope Ratios of TCE, PCE and DCE Isomers by Direct Injection Using CF-IRMS. *Appl.*
339 *Geochemistry* **2006**, *21* (5), 766–781 DOI: 10.1016/j.apgeochem.2006.02.006.
- 340 (29) Aepli, C.; Holmstrand, H.; Andersson, P.; Gustafsson, O. Direct Compound-Specific
341 Stable Chlorine Isotope Analysis of Organic Compounds with Quadrupole GC/MS Using
342 Standard Isotope Bracketing. *Anal. Chem.* **2010**, *82* (1), 420–426 DOI: 10.1021/ac902445f.
- 343 (30) Bernstein, A.; Shouakar-stash, O.; Ebert, K.; Laskov, C.; Hunkeler, D.; Jeannotat, S.;
344 Sakaguchi-s, K.; Laaks, J.; Jochmann, M. A.; Cretnik, S.; Jager, J.; Haderlein, S. B.;

- 345 Schmidt, T. C.; Aravena, R.; Elsner, M. Compound-Specific Chlorine Isotope Analysis: A
346 Comparison of Gas Chromatography/Isotope Ratio Mass Spectrometry and Gas
347 Chromatography/Quadrupole Mass Spectrometry Methods in an Interlaboratory Study.
348 *Anal. Chem.* **2011**, *83*, 7624–7634 DOI: 10.1021/ac200516c |.
- 349 (31) Jin, B.; Laskov, C.; Rolle, M.; Haderlein, S. B. Chlorine Isotope Analysis of Organic
350 Contaminants Using GC-qMS: Method Optimization and Comparison of Different
351 Evaluation Schemes. *environmental Sci. Technol.* **2011**, *45*, 5279–5286 DOI:
352 10.1021/es200749d.
- 353 (32) Sakaguchi-Söder, K.; Jager, J.; Grund, H.; Matthäus, F.; Schüth, C. Monitoring and
354 Evaluation of Dechlorination Processes Using Compound-Specific Chlorine Isotope
355 Analysis. *Rapid Commun. Mass Spectrom.* **2007**, *21* (18), 3077–3084 DOI:
356 10.1002/rcm.3170.
- 357 (33) Doğan-Subaşı, E.; Elsner, M.; Qiu, S.; Cretnik, S.; Atashgahi, S.; Shouakar-Stash, O.; Boon,
358 N.; Dejonghe, W.; Bastiaens, L. Contrasting Dual (C, Cl) Isotope Fractionation Offers
359 Potential to Distinguish Reductive Chloroethene Transformation from Breakdown by
360 Permanganate. *Sci. Total Environ.* **2017**, *596–597*, 169–177 DOI:
361 10.1016/j.scitotenv.2017.03.292.
- 362 (34) Kuder, T.; Van Breukelen, B. M.; Vanderford, M.; Philp, P. 3D-CSIA: Carbon, Chlorine,
363 and Hydrogen Isotope Fractionation in Transformation of TCE to Ethene by a
364 Dehalococcoides Culture. *Environ. Sci. Technol.* **2013**, *47* (17), 9668–9677 DOI:
365 10.1021/es400463p.
- 366 (35) Barth, J. a C.; Slater, G.; Schüth, C.; Bill, M.; Downey, A.; Larkin, M.; Kalin, R. M. Carbon
367 Isotope Fractionation during Aerobic Biodegradation of Trichloroethene by Burkholderia

- 368 Cepacia G4: A Tool to Map Degradation Mechanisms. *Appl. Environ. Microbiol.* **2002**, *68*
369 (4), 1728–1734 DOI: 10.1128/AEM.68.4.1728-1734.2002.
- 370 (36) Chu, K. H.; Mahendra, S.; Song, D. L.; Conrad, M. E.; Alvarez-Cohen, L. Stable Carbon
371 Isotope Fractionation during Aerobic Biodegradation of Chlorinated Ethenes. *Environ. Sci.*
372 *Technol.* **2004**, *38* (11), 3126–3130 DOI: 10.1021/es035238c.
- 373 (37) Clingenpeel, S. R.; Moan, J. L.; McGrath, D. M.; Hungate, B. a.; Watwood, M. E. Stable
374 Carbon Isotope Fractionation in Chlorinated Ethene Degradation by Bacteria Expressing
375 Three Toluene Oxygenases. *Front. Microbiol.* **2012**, *3* (63), 1–7 DOI:
376 10.3389/fmicb.2012.00063.
- 377 (38) Sherwood Lollar, B.; Slater, G. F.; Sleep, B.; Witt, M.; Klecka, G. M.; Harkness, M.;
378 Spivack, J. Stable Carbon Isotope Evidence for Intrinsic Bioremediation of
379 Tetrachloroethene and Trichloroethene at Area 6, Dover Air Force Base. *Environ. Sci.*
380 *Technol.* **2001**, *35* (2), 261–269 DOI: 10.1021/es001227x.
- 381 (39) Bloom, Y.; Aravena, R.; Hunkeler, D.; Edwards, E.; Frape, S. K. Carbon Isotope
382 Fractionation during Microbial Dechlorination of Trichloroethene, Cis -1,2-Dichloroethene,
383 and Vinyl Chloride: Implications for Assessment of Natural Attenuation. *Environ. Sci.*
384 *Technol.* **2000**, *34* (13), 2768–2772 DOI: 10.1021/es991179k.
- 385 (40) Liang, X.; Dong, Y. Distinguishing Abiotic and Biotic Tetrachloroethylene and
386 Trichloroethylene by Stable Carbon Isotope Fractionation. *Environ. Sci. Technol.* **2007**, *41*
387 (20), 7094–7100.
- 388 (41) Wiegert, C.; Mandalakis, M.; Knowles, T.; Polymenakou, P. N.; Aeppli, C.; Macháčková,
389 J.; Holmstrand, H.; Evershed, R. P.; Pancost, R. D.; Gustafsson, O. Carbon and Chlorine
390 Isotope Fractionation during Microbial Degradation of Tetra- and Trichloroethene. *Environ.*

- 391 *Sci. Technol.* **2013**, *47*, 6449–6456 DOI: 10.1021/es305236y.
- 392 (42) Lontoh, S.; Zahn, J. A.; Dispirito, A. A.; Semrau, J. D. Identification of Intermediates of in
393 Vivo Trichloroethylene Oxidation by the Membrane-Associated Methane Monooxygenase.
394 *FEMS Microbiol. Lett.* **2000**, *186* (1), 109–113.
- 395 (43) Fox, B. G.; Borneman, J. G.; Wackett, L. P.; Lipscomb, J. D. Haloalkene Oxidation by the
396 Soluble Methane Monooxygenase from *Methylosinus Trichosporium* OB3b: Mechanistic
397 and Environmental Implications. *Biochemistry* **1990**, *29* (27), 6419–6427 DOI:
398 10.1021/bi00479a013.
- 399 (44) Shuying, L.; Wackett, L. P. Trichloroethylene Oxidation by Toluene Dioxygenase.
400 *Biochem. Biophys. Res. Commun.* **1992**, *185* (1), 443–451 DOI: 10.1016/S0006-
401 291X(05)81005-8.
- 402 (45) Schramm, V. L. Binding Isotope Effects: Boon and Bane. *Curr. Opin. Chem. Biol.* **2007**,
403 *11* (5), 529–536 DOI: 10.1016/j.cbpa.2007.07.013.
- 404 (46) Elsner, M. Stable Isotope Fractionation to Investigate Natural Transformation Mechanisms
405 of Organic Contaminants: Principles, Prospects and Limitations. *J. Environ. Monit.* **2010**,
406 *12* (11), 2005–2031 DOI: 10.1039/c0em00277a.
- 407 (47) Świderek, K.; Paneth, P. Binding Isotope Effects. *Chem. Rev.* **2013**, *113* (10), 7851–7879
408 DOI: 10.1021/cr300515x.
- 409 (48) Renpenning, J.; Rapp, I.; Nijenhuis, I. Substrate Hydrophobicity and Cell Composition
410 Influence the Extent of Rate Limitation and Masking of Isotope Fractionation during
411 Microbial Reductive Dehalogenation of Chlorinated Ethenes. *Environ. Sci. Technol.* **2015**,
412 *49* (7), 4293–4301 DOI: 10.1021/es506108j.
- 413 (49) Renpenning, J.; Keller, S.; Cretnik, S.; Shouakar-stash, O.; Elsner, M.; Schubert, T.;

- 414 Nijenhuis, I.; Jena, D.-. Combined C and Cl Isotope Effects Indicate Differences between
415 Corrinoids and Enzyme (Sulfurospirillum Multivorans PceA) in Reductive Dehalogenation
416 of Tetrachloroethene, But Not Trichloroethene. *Environ. Sci. Technol.* **2014**, *48* (20),
417 11837–11845 DOI: 10.1021/es503306g.
- 418 (50) Wijker, R. S.; Pati, S. G.; Zeyer, J.; Hofstetter, T. B. Enzyme Kinetics of Different Types
419 of Flavin-Dependent Monooxygenases Determine the Observable Contaminant Stable
420 Isotope Fractionation. *Environ. Sci. Technol. Lett.* **2015**, *2* (11), 329–334 DOI:
421 10.1021/acs.estlett.5b00254.
- 422 (51) Mundle, S. O. C.; Spain, J. C.; Lacrampe-Couloume, G.; Nishino, S. F.; Sherwood Lollar,
423 B. Branched Pathways in the Degradation of cDCE by Cytochrome P450 in *Polaromonas*
424 *Sp.* JS666. *Sci. Total Environ.* **2017**, *605–606*, 99–105 DOI:
425 10.1016/j.scitotenv.2017.06.166.
- 426 (52) Pant, P.; Pant, S. A Review: Advances in Microbial Remediation of Trichloroethylene
427 (TCE). *J. Environ. Sci.* **2010**, *22* (1), 116–126 DOI: 10.1016/S1001-0742(09)60082-6.
- 428 (53) Shukla, A. K.; Upadhyay, S. N.; Dubey, S. K. Current Trends in Trichloroethylene
429 Biodegradation: A Review. *Crit. Rev. Biotechnol.* **2014**, *34* (2), 101–114 DOI:
430 10.3109/07388551.2012.727080.
- 431 (54) Farhan Ul Haque, M.; Gu, W.; Baral, B. S.; DiSpirito, A. A.; Semrau, J. D. Carbon Source
432 Regulation of Gene Expression in *Methylosinus Trichosporium* OB3b. *Appl. Microbiol.*
433 *Biotechnol.* **2017**, *101* (9), 3871–3879 DOI: 10.1007/s00253-017-8121-z.
- 434 (55) Lontoh, S.; Semrau, J. D. Methane and Trichloroethylene Degradation by *Methylosinus*
435 *Trichosporium* OB3b Expressing Particulate Methane Monooxygenase. *Appl. Environ.*
436 *Microbiol.* **1998**, *64* (3), 1106–1114.

- 437 (56) Leibman, K. C.; Ortiz, E. Metabolism of Halogenated Ethylenes. *Environ. Health Perspect.*
438 **1977**, *21*, 91–97.
- 439 (57) Newman, L. M.; Wackett, L. P. Fate of 2,2,2-Trichloroacetaldehyde (Chloral Hydrate)
440 Produced during Trichloroethylene Oxidation by Methanotrophs. *Appl. Environ. Microbiol.*
441 **1991**, *57* (8), 2399–2402.
- 442 (58) Maeda, M.; Chung, S. Y.; Song, E.; Kudo, T. Multiple Genes Encoding 2,3-
443 Dihydroxybiphenyl 1,2-Dioxygenase in the Gram- Positive Polychlorinated Biphenyl-
444 Degrading Bacterium *Rhodococcus erythropolis* TA421, Isolated from a Termite
445 Ecosystem. *Appl. Environ. Microbiol.* **1995**, *61* (2), 549–555.
- 446 (59) Medium, M. F. 921 . METHYLOSARCINA QUISQUILLARUM AND
447 https://www.dsmz.de/microorganisms/medium/pdf/DSMZ_Medium921.pdf (accessed Dec
448 12, 2015).
- 449 (60) Elsner, M.; Couloume, G. L.; Lollar, B. S. Freezing to Preserve Groundwater Samples and
450 Improve Headspace Quantification Limits of Water-Soluble Organic Contaminants for
451 Carbon Isotope Analysis. *Anal. Chem.* **2006**, *78* (21), 7528–7534 DOI:
452 10.1021/ac061078m.
- 453 (61) Nikolaou, A. D.; Lekkas, T. D.; Golfinopoulos, S. K.; Kostopoulou, M. N. Application of
454 Different Analytical Methods for Determination of Volatile Chlorination by-Products in
455 Drinking Water. *Talanta* **2002**, *56* (4), 717–726 DOI: 10.1016/S0039-9140(01)00613-0.
- 456 (62) Singleton, D. A.; Merrigan, S. R.; Liu, J.; Houk, K. N. Experimental Geometry of the
457 Epoxidation Transition State. *J. Am. Chem. Soc.* **1997**, *119* (14), 3385–3386 DOI:
458 10.1021/ja963656u.
- 459 (63) Abe, Y.; Aravena, R.; Zopfi, J.; Shouakar-Stash, O.; Cox, E.; Roberts, J. D.; Hunkeler, D.

460 Carbon and Chlorine Isotope Fractionation during Aerobic Oxidation and Reductive
461 Dechlorination of Vinyl Chloride and Cis-1,2-Dichloroethene. *Environ. Sci. Technol.* **2009**,
462 *43* (1), 101–107 DOI: 10.1021/es801759k.

463 (64) Świderek, K.; Paneth, P. Extending Limits of Chlorine Kinetic Isotope Effects. *J. Org.*
464 *Chem.* **2012**, *77* (11), 5120–5124 DOI: 10.1021/jo300682f.

465 (65) Palau, J.; Cretnik, S.; Shouakar-Stash, O.; Höche, M.; Elsner, M.; Hunkeler, D. C and Cl
466 Isotope Fractionation of 1,2-Dichloroethane Displays Unique $\delta^{13}\text{C}/\delta^{37}\text{Cl}$ Patterns for
467 Pathway Identification and Reveals Surprising C-Cl Bond Involvement in Microbial
468 Oxidation. *Environ. Sci. Technol.* **2014**, *48*, 9430–9437 DOI: 10.1021/es5031917.

469 (66) Cretnik, S.; Bernstein, A.; Shouakar-Stash, O.; Löffler, F.; Elsner, M. Chlorine Isotope
470 Effects from Isotope Ratio Mass Spectrometry Suggest Intramolecular C-Cl Bond
471 Competition in Trichloroethene (TCE) Reductive Dehalogenation. *Molecules* **2014**, *19* (5),
472 6450–6473 DOI: 10.3390/molecules19056450.

473 (67) Siwek, A.; Omi, R.; Hirotsu, K.; Jitsumori, K.; Esaki, N.; Kurihara, T.; Paneth, P. Binding
474 Modes of DL-2-Haloacid Dehalogenase Revealed by Crystallography, Modeling and
475 Isotope Effects Studies. *Arch. Biochem. Biophys.* **2013**, *540* (1–2), 26–32 DOI:
476 10.1016/j.abb.2013.09.012.

477 (68) Audí-Miró, C.; Cretnik, S.; Otero, N.; Palau, J.; Shouakar-Stash, O.; Soler, A.; Elsner, M.
478 Cl and C Isotope Analysis to Assess the Effectiveness of Chlorinated Ethene Degradation
479 by Zero-Valent Iron: Evidence from Dual Element and Product Isotope Values. *Appl.*
480 *Geochemistry* **2013**, *32*, 175–183 DOI: 10.1016/j.apgeochem.2012.08.025.

481
482

